# FAST AND EXPRESSIVE MULTI-TOKEN PREDICTION WITH PROBABILISTIC CIRCUITS

Andreas Grivas\* Lorenzo Loconte\* Emile van Krieken\* Piotr Nawrot\* Yu Zhao\*

Euan Wielewski<sup>♦</sup> Pasquale Minervini\* Edoardo Ponti\* Antonio Vergari\*

\*School of Informatics, University of Edinburgh \quat \text{NatWest Group}

#### **ABSTRACT**

Multi-token prediction (MTP) is a prominent strategy to significantly speed up generation in large language models (LLMs), including byte-level LLMs, which are tokeniser-free but prohibitively slow. However, existing MTP methods often sacrifice expressiveness by assuming *independence* between future tokens. In this work, we investigate the trade-off between expressiveness and latency in MTP within the framework of probabilistic circuits (PCs). Our framework, named MTPC, allows one to explore different ways to encode the joint distributions over future tokens by selecting different circuit architectures, generalising classical models such as (hierarchical) mixture models, hidden Markov models and tensor networks. We show the efficacy of MTPC by retrofitting existing byte-level LLMs, such as EvaByte. Our experiments show that, when combined with speculative decoding, MTPC significantly speeds up generation compared to MTP with independence assumptions, while guaranteeing to retain the performance of the original verifier LLM. We also rigorously study the optimal trade-off between expressiveness and latency when exploring the possible parameterisations of MTPC, such as PC architectures and partial layer sharing between the verifier and draft LLMs.

# 1 Introduction

Autoregressive (AR) large language models (LLMs) can only perform single-token prediction (STP) as they generate one token at a time, incurring significantly high latency, energy demand, and deployment costs. This affects not only subword models, but even more so the byte-level ones (Yu et al., 2023; Wang et al., 2024, *inter alia*). Among possible alternatives to speed up generation (Ankner et al., 2024; DeepSeek-AI et al., 2024; Nawrot et al., 2023; Pagnoni et al., 2024; Łańcucki et al., 2025), multi-token prediction (MTP) stands out as it promises to predict a window of multiple tokens *all at once*, may they be subwords (Gloeckle et al., 2024; Cai et al., 2024) or bytes (Gloeckle et al., 2024; Zheng et al., 2025). As such, MTP LLMs can achieve a significantly higher throughput than STP ones, as they decrease the number of forward passes required through the LLM.

Nevertheless, modelling the joint distribution over all future tokens in a window is challenging, as it requires balancing *expressiveness*, i.e., representing all the dependencies between tokens, and *efficiency*, i.e., minimising latency. Existing MTP approaches favour the latter by making an unrealistic assumption: namely, considering all future tokens to be independent (Zheng et al., 2025; Cai et al., 2024; Gloeckle et al., 2024). This clearly comes at the expense of expressiveness (Ankner et al., 2024; Wertheimer et al., 2024), as the choice of a token for a position within the window cannot influence the probability of the others.

For example, consider the prompt: "Name a capital of South Africa", where Cape Town and Pretoria are equally likely completions. A byte-level MTP model with independence assumptions over an 8-token window could return Cretoria as an argmax, because replacing P with C cannot change the probability of other tokens. More concerningly, an exponential number of "byte-salad" continuations, such as Crptoria, Crpt ria and Crpt roa, are then also equally likely, despite having almost zero probability under the STP model. Recently, Basharin et al. (2025) introduced dependencies into MTP

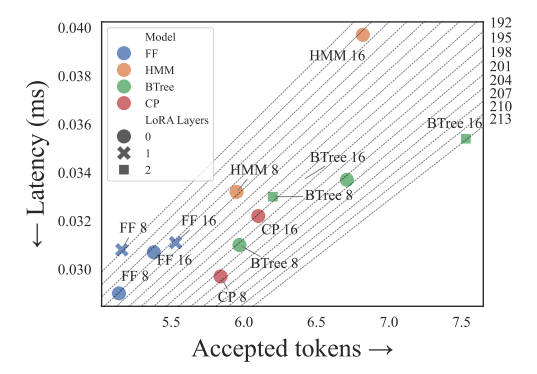


Figure 1: MTPC allows for exploring the trade-off between efficiency (latency) and expressiveness (token acceptance) with different MTP designs in terms of 1) choice of PC architecture (FF, CP, HMM, BTree); 2) choice of layers shared between draft and verifier models in self-speculative decoding. Dotted lines indicate iso-throughput (tokens generated per second) regions, highlighting configurations such as BTree for n=16 tokens and 2 LoRA layers that achieve the best throughput.

with a mixture over the future token probabilities. However, a single mixture can only add limited expressiveness. Crucially, understanding how to increase expressiveness while optimally trading off efficiency in a systematic way is still an open question.

In this paper, we fill this gap by proposing an MTP framework based on probabilistic circuits (PCs; Choi et al., 2020; Vergari et al., 2021), which we name MTPC. MTPC uses PCs to parameterise the joint distribution over future tokens into tractable computational graphs that can encode hierarchical mixture models. As such, MTPC offers a way to systematically navigate the spectrum of MTP architectural variants, encompassing fully factorised models (Zheng et al., 2025; Cai et al., 2024; Gloeckle et al., 2024) and shallow mixtures (Basharin et al., 2025) but also more expressive parameterisations: hidden Markov models (HMMs) and binary tree factorisations (BTrees) which are novel for MTP.

Moreover, in contrast to previous work on MTP (Zheng et al., 2025; Cai et al., 2024), MTPC guarantees we match the quality of an AR LLM via speculative decoding (Leviathan et al., 2022; Chen et al., 2023; Stern et al., 2018; Xia et al., 2024)—exactly for greedy decoding or in expectation for sampling—showing that the throughput sacrificed for the guarantee is not as large as alluded to previously. We do so by sharing the LLM backbone for the draft and verifier models for different numbers of layers, highlighting how this creates *a second dimension to trade-off expressiveness* (as hidden representations between draft and verifier can diverge) *and latency* (as each non-shared layer requires separate forward passes). We illustrate the two trade-offs at the core of MTPC in Fig. 1.

In summary, we make the following contributions: C1) we introduce MTPC, a fast MTP framework based on PCs that overcomes the independence assumptions of previous work and generalises tensor decomposition methods (Basharin et al., 2025); C2) we rigorously identify trade-offs between acceptance rates in speculative decoding and latency of generation, based on different choices of probabilistic circuit (PC) architectures and partial layer sharing; C3) we empirically demonstrate the effectiveness of MTPC by repurposing EvaByte (Zheng et al., 2025), a byte-level LLM, into our framework. The choice of this use case is motivated by the fact that existing byte-level LLMs (Pagnoni et al., 2024; Wang et al., 2024) obviate the limitations of sub-word tokenisers—including uneven efficiency (Ahia et al., 2023; Dagan et al., 2024), lack of interoperability (Minixhofer et al., 2025), and vulnerabilities (Rumbelow & Watkins, 2023; Land & Bartolo, 2024; Geiping et al., 2024; Salesky et al., 2021)—at the cost of significantly slowing down generation. We find that MTPC increases the throughput of EvaByte by 5.47× with respect to AR generation and 1.22× with respect to MTP with independence assumptions.

# 2 Speeding up Generation with MTP and Speculative Decoding

Given our goal of speeding up LLM generation with MTP while guaranteeing that the STP quality is fully retained through speculative decoding, we introduce these frameworks below.<sup>1</sup>

**MTP.** A classical STP LLM encodes a distribution over sequences of tokens  $\{\mathbf{x}_t\}$  defined over a vocabulary  $\mathcal{V}$  as  $\prod_t p(x_{t+1} \mid \mathbf{x}_{\leq t})$ , where  $\mathbf{x}_{\leq t}$  is the context, *i.e.* the observed tokens at timestep t. MTP (Gloeckle et al., 2024) aims to extend an STP LLM that predicts a single token at a time through  $p(x_{t+1} \mid \mathbf{x}_{\leq t})$ , to an MTP model,  $q_{\boldsymbol{\theta}}$ , that models the *joint* probability of a window of n

<sup>&</sup>lt;sup>1</sup>We adapt notation from the tensor and circuit literature (Loconte et al., 2025a), see Section A.

future tokens and generates them simultaneously, i.e.,

$$q_{\theta}(x_{t+1}, x_{t+2}, \dots, x_{t+n} \mid \mathbf{x}_{\leq t}).$$
 (1)

where  $\boldsymbol{\theta}$  denotes a given parameterisation for the joint. The first dimension to trade-off expressiveness and efficiency in MTP pertains to compactly representing  $q_{\boldsymbol{\theta}}$ . Unlike for  $p(x_{t+1} \mid \mathbf{x}_{\leq t})$ , we would need to store more than a vector of logits  $\mathbf{a} \in \mathbb{R}^v$  of a single univariate categorical distribution for a vocabulary size  $v = |\mathcal{V}|$  for every timestep t. The most expressive, but least efficient way to do so, would be to store an n-dimensional tensor  $\boldsymbol{\mathcal{A}} \in \mathbb{R}^{v^{(1)} \times \ldots \times v^{(n)}}$  of logits having  $v^n$  entries, but this scales exponentially in n. Next, we review past attempts to avoid storing  $\boldsymbol{\mathcal{A}}$  explicitly.

**Fully factorised.** The most commonly used way to boost efficiency is to assume all n future tokens are independent (Zheng et al., 2025; Cai et al., 2024; Gloeckle et al., 2024), that is,  $q_{\theta}$  factorizes as

$$\prod_{i=1}^{n} q_{\phi_i}(x_{t+i} \mid \mathbf{x}_{\leq t}). \tag{FF}$$

This comes with the benefit that one needs to store only n v-dimensional vectors of probabilities  $\phi_i$  to represent the joint distribution in Eq. (1). At the same time, as already discussed in the introduction, this severely limits model expressiveness (Ankner et al., 2024; Wertheimer et al., 2024).

Canonical polyadic (CP) factorisation. Dependencies between future tokens can be recovered by introducing explicit latent variables (Lee et al., 2018). To this end, Basharin et al. (2025) propose to factorise Eq. (1) via an r-rank CP decomposition. A CP decomposition introduces one discrete latent variable, Z, that encodes a mixture of r fully-factorised components, rewriting Eq. (1) as:

$$\sum_{j=1}^{r} q(Z=j \mid \mathbf{x}_{\leq t}) \prod_{i=1}^{n} q_{\phi_{i,j}}(x_{t+i} \mid j, \, \mathbf{x}_{\leq t}).$$
 (CP)

where  $q(j \mid \mathbf{x}_{\leq t}) = \omega_j$  are the mixture coefficients and  $\phi_{i,j}$  are the parameters of the categorical distribution for mixture component j at position i in the MTP window. <sup>3</sup> Before showing how we can generalize both FF and CP MTP with PCs, we review how to ensure MTP models match the quality of a given STP model.

**Speculative decoding** (Stern et al., 2018; Leviathan et al., 2022; Chen et al., 2023; Xia et al., 2024) can be combined with MTP to speed up generation while guaranteeing no loss in quality. Given a target STP LLM that we wish to accelerate, speculative decoding involves two steps: 1) *drafting*, where a cheaper MTP draft model generates n future tokens, and 2) *verification*, where the target STP model accepts or rejects the generated tokens in parallel according to a pre-defined consistency criterion. The closer the distributions of the draft and verifier are, the more often 'speculated' tokens are accepted, speeding up generation. With speculative decoding we can quantify the trade-off between expressivenss and efficiency in MTP models as their *throughput*, i.e.

where acceptance rates are a function of the total variation distance between the two distributions (Leviathan et al., 2022; Sun et al., 2023) and latency measures how computationally expensive an MTP model is during generation. While previous work, such as Basharin et al. (2025), focused only on measuring acceptance rates, we highlight how both sides of the ratio in Eq. (2) are important, as they create a spectrum. MTPCs provide a systematic way to navigate such a spectrum (see Fig. 1).

## 3 PROBABILISTIC CIRCUITS FOR MULTI-TOKEN PREDICTION

The idea behind MTPCs is to further decompose the joint distribution in Eq. (1) into a deep computational graph encoding a hierarchical mixture model, called a *probabilistic circuit* (Sections 3.1 and 3.2), and to parameterise it with LLM embeddings (Section 3.3).

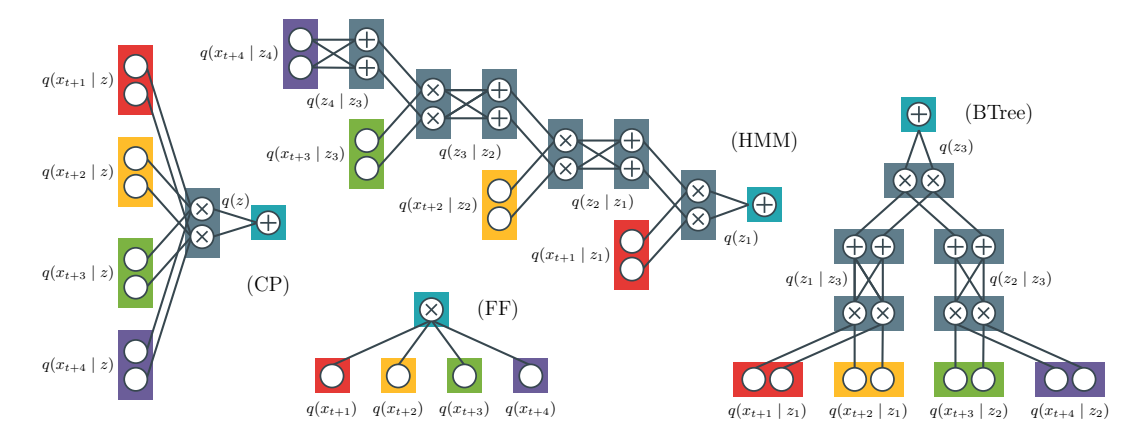


Figure 2: **PCs allow for modelling a spectrum of dependency structures** over sequences of tokens, as shown for the known FF and CP and the novel HMM and BTree MTP variants. Input units are grouped in coloured layers, one for each token, while sum and product layers encoding (hierarchies of) latent variable distributions are in grey. The output unit of each circuit (in blue) computes  $q_{\theta}(x_{t+1}, \dots, x_{t+n} \mid \mathbf{x}_{< t})$ . In the figure we omit the dependency on the context  $\mathbf{x}_{< t}$  for readability.

#### 3.1 PROBABILISTIC CIRCUITS

A *circuit* (Darwiche, 2003; Choi et al., 2020; Vergari et al., 2021), c, is a parameterised directed acyclic computational graph<sup>4</sup> over variables  $\mathbf{X}$  encoding a function,  $c(\mathbf{X})$ , and comprises three kinds of computational units: *input*, *product*, and *sum* units. Each product or sum unit n receives the outputs of other units as inputs, denoted with the set in(n). Each unit n encodes a function,  $c_n$ , defined as: (i)  $c_n(\mathsf{sc}(n);\phi)$  if n is an input unit, where  $c_n$  is a function parameterised by  $\phi$  over variables  $\mathsf{sc}(n) \subseteq \mathbf{X}$ , called its scope; (ii)  $\prod_{j \in \mathsf{in}(n)} c_j(\mathsf{sc}(j))$  if n is a product unit; and (iii)  $\sum_{j \in \mathsf{in}(n)} \omega_j c_j(\mathsf{sc}(j))$  if n is a sum unit, with  $\omega_j \in \mathbb{R}$  denoting the sum parameters. The scope of a product or sum unit n is the union of the scopes of its inputs, i.e.,  $\mathsf{sc}(n) = \bigcup_{j \in \mathsf{in}(n)} \mathsf{sc}(j)$ . Fig. 2 shows examples of circuits, where units of the same scope are grouped into (coloured) layers belonging to a hierarchy that can be easily parallelised on a GPU (Mari et al., 2023; Loconte et al., 2025a).

For MTPCs, we use *probabilistic circuits* (PCs), i.e., circuits modelling a joint distribution over random variables, in our case tokens  $\mathbf{X} = \{X_1, \dots, X_n\}$ . PCs encode Eq. (1) as

$$q_{\theta}(x_{t+1}, \dots, x_{t+n} \mid \mathbf{x}_{\leq t}) = Z_{\theta_t}^{-1} c(x_{t+1}, \dots, x_{t+n}; \theta_t)$$
 (3)

where  $\theta_t = \{\omega_t, \phi_t\}$  denote the set of circuit parameters, i.e., all sum unit parameters  $\omega_t$  and input unit parameterisations  $\phi_t$  which depend on the context  $\mathbf{x}_{\leq t}$ ; and  $Z_{\theta_t}$  denotes the partition function of c, i.e.,  $Z_{\theta_t} = \sum_{x_{t+1},\dots,x_{t+n}\in\mathcal{V}^n} c(x_{t+1},\dots,x_{t+n};\theta_t)$ . Note that the PC architectures we are interested in are already normalised or always allow computing the partition function in a single feedforward step (see Choi et al. (2020) and Section B.1). At the same time, we can easily sample from PCs in a single feedforward pass, as discussed in Section B.2. Crucially, within the framework of PCs, we can recover the FF and CP parameterisations for MTP and several other architectures that generalise tensor factorisations (Loconte et al., 2025a) that can be used as novel MTP models, each offering a different expressiveness-efficiency trade-off. We do so while abstracting away from each model's original formulation and obtain a unified way to parameterise MTP LLMs, as discussed next.

 $<sup>^{2}</sup>$ These parameters depend on t, we drop the subscript when not needed to avoid clutter.

<sup>&</sup>lt;sup>3</sup>Basharin et al. (2025) calls CP a mixture of experts (MoE), but we note this is incorrect as the weights  $\omega_j$  do not depend on future tokens, but only on past ones. As such, they realise a simple conditional mixture. They argue that training CP is challenging and requires insights from the MoE literature, while we are able to train them as well as deeper mixture variants easily without MoE-tailored losses (see Section 4).

<sup>&</sup>lt;sup>4</sup>In Fig. 2, edges directionality is removed for readability, but it is assumed to be from inputs to outputs.

# 3.2 PC ARCHITECTURES FOR MTP

**MTPC-FF.** Representing the commonly used FF MTP parameterisation as a PC is simple: we introduce n input units, each parameterised by  $\phi_i$ , its corresponding token probabilities, and connect them all to a single product unit, as shown in Fig. 2 for a distribution over n=4 tokens.

MTPC-CP. Similarly, we can easily encode a CP factorisation in a *shallow* PC by i) introducing r input units for each token (each parameterised by their own probabilities  $\phi_{ij}$ ), then ii) multiplying them to retrieve the r factorised mixture components, which we then iii) aggregate in a sum unit with weights  $\omega_j = q(z_j \mid \mathbf{x}_{\leq t})$  (see also Proposition 1 in Loconte et al. (2025a)). Fig. 2 shows this construction for n=4 and r=2. This basic construction suggests that we can create deeper architectures by interleaving sum and product layers, while overparameterising each layer by increasing the number of units in it (r). Furthermore, by implementing CP as a PC unlocks a faster sampling routine (Section B.2) than the one used in Basharin et al. (2025).

MTPC-HMM. As a further example of the expressiveness increase we get by generalising our approach to deeper PCs, we introduce a factorisation that realises a hidden Markov model (HMM), which better captures distant dependencies in the sequence by introducing a sequence of latent variables, in contrast to the single one present in CP. More precisely, we define an HMM with r hidden states and truncate its prediction window to n steps into the future. We resort to an inhomogeneous HMM, i.e., we do not make the transition matrices time-invariant, as this setup is more expressive and worked better in our experiments, see Section E. This simplifies Eq. (1) into:

$$\sum_{z_1=1}^r \cdots \sum_{z_n=1}^r q(z_1 \mid \mathbf{x}_{\leq t}) q_{\phi}(x_{t+1} \mid z_1, \mathbf{x}_{\leq t}) \prod_{i=2}^n q(z_i \mid z_{i-1}, \mathbf{x}_{\leq t}) q_{\phi}(x_{t+i} \mid z_i, \mathbf{x}_{\leq t}).$$
 (HMM)

Fig. 2 illustrates the HMM parameterisation above represented as a circuit, comprising n=4 pairs of sum and product layers stacked, where the parameters  $\omega_i$  of the former are the transition probabilities  $q(z_i \mid z_{i-1}, \mathbf{x}_{\leq t})$ . Similarly to CP, we can increase r to overparameterise the circuit with more input units per token and sum units overall, and hence increase expressiveness.

MTPC-BTREE. One drawback of the HMM parameterisation is the asymmetry of its computational graph, which i) provides fewer latent variables for the early tokens, and ii) increases latency when predicting the last tokens due to its autoregressive token dependencies. To solve this, we build a PC whose structure resembles that of a binary tree (BTree), effectively encoding a hierarchy of latent variables or a tree tensor factorisation (Grasedyck, 2010; Cheng et al., 2019; Loconte et al., 2025a). This is done recursively: at each step h of the hierarchy, given a sequence of n tokens to split, and a parent latent variable  $Z_l$ , we split it into two sub-sequences  $(x_{t+1}, \ldots, x_{t+\lfloor n/2 \rfloor - 1})$  and  $(x_{t+\lfloor n/2 \rfloor}, \ldots, x_{t+n})$ , then factorise Eq. (1) as a mixture:

$$\sum_{z_h=1}^r q(z_h \mid z_l, \mathbf{x}_{\leq t}) q_{\boldsymbol{\theta}}(x_{t+1}, \dots, x_{t+\lfloor n/2 \rfloor - 1} \mid z_h, z_l, \mathbf{x}_{\leq t}) q_{\boldsymbol{\theta}}(x_{t+\lfloor n/2 \rfloor}, \dots, x_{t+n} \mid z_h, z_l, \mathbf{x}_{\leq t})$$
(BTree)

which corresponds to creating a sum unit whose weights are  $q(z_h \mid z_l, \mathbf{x}_{\leq t})$  followed by products. We repeat the process while caching intermediate units until we reach the base case for n=1, for which we create a layer of input units for the corresponding token. Fig. 2 illustrates the BTree circuit built in this way. Our experiments (Section 4.2) show that the BTree parameterisation obtains the optimal throughput by lowering the latency of HMM, as it samples more latent variables and tokens in parallel, while achieving similar acceptance rates.

#### 3.3 PARAMETERISING PCs WITH LLMs

Parameterising MTPCs requires two functions: an LLM that maps the context  $\mathbf{x}_{\leq t} \in \mathcal{V}^t$  into contextual features, and a neural network head that maps the contextual features to the parameters of the circuit  $\boldsymbol{\theta}_t$ , realising a *neural conditional circuit* (Shao et al., 2020; 2022). To extract the contextual features  $\mathbf{e}_t \in \mathbb{R}^d$ , we use  $\mathbf{e}_t = \mathrm{LLM}_{\mathrm{LoRA}(k)} (\mathbf{x}_{\leq t})$  where  $\mathrm{LLM}_{\mathrm{LoRA}(k)} \colon \mathcal{V}^t \to \mathbb{R}^d$  is the STP backbone with LoRA (Hu et al., 2022) applied to the last  $k \geq 0$  layers. As we will discuss in Section 4.4, the number of LoRA layers can impact throughput significantly. Given  $\mathbf{e}_t$ , we realise Eq. (3) by computing  $\boldsymbol{\theta}_t = g_c(\mathbf{e}_t)$ , where  $g_c$  is a neural network head that outputs both the input unit parameters,  $\boldsymbol{\phi}_t$ , and the sum unit parameters,  $\boldsymbol{\omega}_t$  (Section 3.1). Note that our parameterisation in

MTPCs allows us to abstract from the actual structure of the circuit (i.e., FF, CP, HMM or BTree) and just focus on these two sets of tensorised parameters, as we discuss next.

Input unit distributions. All MTPCs produce joint distributions over token windows by combining categorical distributions over individual tokens (Fig. 2). We follow EvaByte (Zheng et al., 2025) and learn n separate unembedding layers, one per window position. For models with mixture coefficients, we also learn one unembedding layer per mixture coefficient. As such, instead of a single unembedding matrix mapping  $\mathbb{R}^d \to \mathbb{R}^v$ , we have an unembedding tensor  $\mathcal{W} \in \mathbb{R}^{n \times r \times v \times d}$ , and compute the input distributions with the usual unembedding operation followed by softmax, i.e.,  $\phi_{tij} = \operatorname{softmax}(\mathcal{W}_{ij}e_t)$ , where i and j index the position in the MTP window and the rank r.

Sum unit parameters. For sum units, instead of mapping embeddings to the vocabulary via  $\mathcal{W}$ , we map to the rank of the sum unit via  $\mathcal{R} \in \mathbb{R}^{z \times r \times d}$ , where z is the number of sum units, r is its rank, and d the dimensionality of  $\mathbf{e}_t$ . We compute  $\omega_{ti} = \operatorname{softmax}(\mathcal{R}_i \mathbf{e}_t)$ , where i indexes the sum unit.

## 3.4 Speculative Decoding with MTPC

For MTPCs, we design an architecture that is *self-drafting* (Zhang et al., 2024b; Cai et al., 2024), i.e. where the draft and verifier models share the same LLM backbone. We use an MTP head (Cai et al., 2024; Ankner et al., 2024) augmented with our circuits to efficiently sample a draft, and an autoregressive STP head as the verifier. Optionally, we also explore keeping a few final transformer layers separate in the two models by fine-tuning LoRA adaptors for the draft model's backbone.

Unlike previous self-drafting MTP works (Cai et al., 2024; Ankner et al., 2024), we guarantee that the generated tokens are the same as those the autoregressive LLM would generate in expectation by using *speculative decoding* (Leviathan et al., 2022; Chen et al., 2023), *i.e.*, we only generate the subset of drafted tokens accepted by our verifier. To keep latency low, we make only a single LLM call per speculative decoding cycle by re-using the LLM backbone state computed by the verifier for the draft model, where possible. We achieve this by modifying the speculative decoding algorithm slightly, as we detail in Algorithm 2.

Next we report results for sampling, but we also experimented with greedy speculative decoding (Stern et al., 2018) which guarantees argmax consistency. Both are suitable for MTPCs.

# 4 MTPCs in Action: Retrofitting a Byte-Level LLM

We evaluate MTPC on the challenging tasks of speeding up byte-level LLMs. MTP is crucial for byte-level LLMs as they require more tokens than sub-word LLMs to generate text with the same length. Furthermore, byte-level LLMs allow us to explore large window sizes and more mixtures components due to their small vocabulary size. We implement our MTPCs variants in the cirkit library (The april Lab, 2024) and provide it in our supplementary materials.

**Target model.** We work with EvaByte (Zheng et al., 2025) as our byte-level LLM, because it is open source, publicly available, and obtains results that are competitive to subword-level LLMs on benchmarks (Zheng et al., 2025). EvaByte is a 6.5B byte-level model with an embedding size of 4096, a vocabulary of 320 byte tokens and a maximum context window of 32k bytes. EvaByte has been pre-trained as an MTP model with a prediction window of n = 8 bytes. In our experiments, we retrofit the released fine-tuned version of EvaByte, EvaByte-SFT (Zheng et al., 2025). EvaByte-SFT has been fine-tuned on a data mix of Tülu 3 (Lambert et al., 2024), OpenCoder (Huang et al., 2024) stages one and two, and OpenHermes 2.5. We note that EvaByte's solid performance on benchmarks is based on greedy decoding when the model is used for STP, which we name EvaByte-STP. For this reason, we set EvaByte-STP as the target model for speculative decoding. We do so to accelerate generation without sacrificing generation quality.

**Draft models.** We use EvaByte-MTP to refer to EvaByte's released fully-factorised (FF) MTP head. Speculative decoding results have not been reported in the EvaByte release (Zheng et al., 2025), so we include them here as our baseline. We also further fine-tune EvaByte-MTP to highlight that the model cannot be improved further. On top of that, we replace the MTP head with our MTPCs

<sup>&</sup>lt;sup>5</sup>This is efficient even for PCs with high rank due to the small vocabulary size of byte-level LLMs.

<sup>&</sup>lt;sup>6</sup>The information above is from personal communication with the authors.

heads, including our CP implementation and novel HMM and BTree heads to relax the independence assumptions of the FF model and increase expressiveness. We note that EvaByte-MTP-CP with r=1 is equivalent to EvaByte-MTP, as can be seen from Eq. (CP).

#### 4.1 Training

In order to improve throughput via speculative decoding, we need to make our MTP model's distribution as similar as possible to EvaByte-STP's. We achieve this in the simplest way by instruction fine-tuning our models on a similar data mix to that used for EvaByte-SFT. As the full details of the data mix are not known and are hard to replicate, we focus on Tülu 3.

**Training data.** We fine-tune on the Tülu 3 SFT mix dataset (Lambert et al., 2024) which contains 939,344 examples of user/assistant interactions on 18 tasks. We split the Tulu 3 dataset into training and validation so that we can check throughput on the unseen validation examples. In order to make sure all tasks are sampled, we shuffle the training data before splitting. Because we want training to be possible on  $2 \times 80$  Gb GPUs, we limit the context length to 8192 bytes and filter out 34,067 examples which are longer. We split the remaining 905,277 examples into 99% train and 1% validation.

**Initialisation.** We initialise our MTP heads from EvaByte-SFT in a way that guarantees that our EvaByte-MTP-CP is equivalent to EvaByte-MTP. This guarantees that we leverage previous training: all models start from the same loss and we smoothly move in parameter space from EvaByte-MTP to our more expressive EvaByte-MTP-CP, EvaByte-MTP-HMM and EvaByte-MTP-BTree.

**Loss.** We train our MTP models on the packed train split of Tülu 3 with a batch size of 256 sequences, or  $\approx 2$ m tokens, which is what EvaByte used. We first train our MTP heads for 1 epoch (Section 4.3). Then we load the models and continue training for an additional epoch with LoRA (Section 4.4). We apply EvaByte's chat template and only train on the assistant's answers. We use overlapping prediction windows, as we need to be able to begin speculative decoding from any position during generation. We minimise the negative log-likelihood of the observed assistant outputs Eq. (4), where N is the number of training sequences and L is the sequence length for each token in the window.

$$\mathcal{L} = \sum_{j=1}^{n} \gamma^{j-1} \mathcal{L}_{j}, \quad \mathcal{L}_{j} = -\sum_{i=1}^{N} \sum_{t=1}^{L} (\log p_{\theta}(x_{t+j}^{(i)} \mid \mathbf{x}_{< t+j}^{(i)})) / (N \text{valid}(i, j))$$
(4)

This involves locally normalising the loss by the number of valid tokens for example i and output j in the MTP window, valid(i,j). As in Cai et al. (2024), we apply exponential discounting for future tokens in the window, but use  $\gamma=0.9$  instead of  $\gamma=0.8$  to account for n>8. We use the Adam optimiser (Kingma & Ba, 2015) with a fixed learning rate of  $3\times 10^{-4}$ .

#### 4.2 METRICS

To speed up LLMs generation with speculative decoding, we need to balance **speed** and **expressiveness**. We measure speed using **mean latency** ( $\mu_{lat}$ ) and expressiveness via the **mean acceptance rate** ( $\mu_{acc}$ ; Li et al., 2024), as defined below. Our goal is to increase **throughput**. We obtain a relative throughput speed-up of one method over another by measuring their **wall-time speedup ratio** (Li et al., 2024; Cai et al., 2024). We assume a batch size of 1 for all evaluations. We report our metrics on two GPUs, the server-grade NVIDIA L40S GPU and the desktop-grade NVIDIA RTX 3090.

**Mean Latency**  $\mu_{\text{lat}}$  is the average time taken for each speculative decoding step, *i.e.*, the time needed for the draft model to generate a candidate sequence and the verifier to choose which tokens to accept.  $\mu_{\text{lat}}$  is higher for less efficient LLMs and MTP heads, and lower for more powerful GPUs, *e.g.* for EvaByte-MTP the L40S (Tables 1 to 3) has half the latency of the RTX 3090 (Tables 4 to 6).

**Mean acceptance rate**  $\mu_{\rm acc}$  is the percentage of drafted tokens that are accepted by the target model. More expressive draft models will have higher accepance rate as they will better approximate the target distribution.  $\mu_{\rm acc}$  depends on the size of the MTP window, n, as we have  $\mu_{\rm acc} \in [0, n]$ .

**Mean throughput**  $\mu_{\text{tok/s}}$  is measured as in Eq. (2), i.e., as the ratio  $\mu_{\text{acc}}/\mu_{\text{lat}}$ .

**Wall-time speed-up ratio** is the relative speed-up of a proposed model compared to a baseline model, measured as the ratio of their throughputs. As baselines, we use autoregressive generation from the STP model, EvaByte-STP, and MTP with independence assumptions, EvaByte-MTP FF.

Our loss over overlapping windows is a composite log-likelihood (Varin et al., 2011).

model	r	$\mu_{ m acc}$ $\uparrow$	$\mu_{\mathrm{lat}}\downarrow$	$\mu_{ ext{tok/s}} \uparrow$	max <sub>tok/s</sub>
FF	1	$5.14 \pm 0.06$	$0.0290 \pm 0.0002$	$180.1 \pm 2.8$	297.50
	8	$5.65 \pm 0.02$	$0.0296 \pm 0.0001$	$194.5 \pm 1.6$	291.61
	16	$5.76 \pm 0.03$	$0.0299 \pm 0.0002$	$196.1 \pm 1.9$	295.94
CP	32	$5.84 \pm 0.01$	$0.0297\pm 0.0002$	$200.9 \pm 1.6$	292.33
	64	$5.87 \pm 0.09$	$0.0304 \pm 0.0001$	$197.2 \pm 2.3$	278.42
	128	$\textbf{5.94} \pm 0.04$	$0.0320\pm 0.0001$	$188.6 \pm 1.1$	265.51

Table 1: Increasing the mixture components (r) increases the throughput  $(\mu_{\text{tok/s}})$  as seen for MTPC-CP (n=8) over our baseline, EvaByte-MTP (FF) (in gray) where we report the mean  $\pm$  std over three sets of 250 prompts. MTPC-CP increases throughput: it has a larger acceptance rate  $(\mu_{\text{acc}})$  while latency  $(\mu_{\text{lat}})$  is almost constant in r.

$\overline{n}$	r	model	$\mu_{ m acc}$ $\uparrow$	$\mu_{\mathrm{lat}}\downarrow$	$\mu_{ ext{tok/s}}$ $\uparrow$	speed-up ↑
1	1	STP	_	0.0251	40.03	1.00
	1	FF	$5.14 \pm 0.06$	$0.0290 \pm 0.0002$	$180.1 \pm 2.8$	4.50
8	32	HMM	$5.95 \pm 0.05$	$0.0332 \pm 0.0001$	$182.4 \pm 0.9$	4.56
0	32	BTree	$5.97 \pm 0.06$	$0.0310 \pm 0.0004$	$196.6 \pm 3.8$	4.91
	32	CP	$5.84 \pm 0.01$	$0.0297\pm 0.0002$	$200.9 \pm 1.6$	5.02
	1	FF	$5.38 \pm 0.08$	$0.0307 \pm 0.0004$	$179.6 \pm 3.8$	4.49
16	32	HMM	$6.82 \pm 0.04$	$0.0397 \pm 0.0001$	$174.5 \pm 0.7$	4.36
10	32	CP	$6.10 \pm 0.05$	$0.0322 \pm 0.0001$	$193.4 \pm 1.8$	4.83
	32	BTree	$6.71 \pm 0.01$	$0.0337 \pm 0.0000$	$203.5 \pm 0.1$	5.08

Table 2: More expressive architectures such as MTPC-BTREE outperform MTPC-CP in terms of throughput for n=8 and n=16 windows on an L40S GPU. For this experiment, we trained only model heads (no LoRAs layers). The shaded baselines are EvaByte-STP and the EvaByte-MTP (FF) models, trained for the same number of steps as our circuits for a fair comparison.

#### 4.3 MTPCs WITHOUT ADAPTERS

**RQ1**: Can we increase throughput by increasing the number of mixture components?

We begin with the simplest PC from our framework, MTPC-CP, which relaxes the independence assumption of the widely used MTPC-FF (r=1) by increasing the number of mixture coefficients, r. MTPC-CP can increase throughput because it is more expressive yet still very efficient.

Table 1 highlights MTPC-CP's efficiency; the  $\mu_{\rm lat}$  introduced by MTPC-CP remains relatively unchanged as we increase r, because the forward pass cost of the output layer is dominated by the expensive LLM calls. At the same time, MTPC-CP increases the expressiveness of our MTP head by relaxing the unrealistic independence assumptions. As a result, MTPC-CP with r=128 achieves  $\mu_{\rm acc}=5.94$ , an increase of .82 tokens over MTPC-FF. However, the best throughput is obtained for r=32, where MTPC-CP produces 20.8 more tok/s than MTPC-FF. In the last column, we show the maximum attainable throughput (max<sub>tok/s</sub>), i.e., we disable speculative decoding and accept all tokens. The price paid in throughput for guaranteeing no loss in generation quality is  $\approx 90$  tok/s for r=32. While MTPC-CP performs well for n=8, the margin for further improving throughput is small. This is because for n=8, we can at best achieve  $\mu_{\rm acc}=8$ , and we have already achieved  $\mu_{\rm acc}=5.94$  and have hit diminishing returns. To obtain substantial boosts in throughput, we need to extend our model to longer window sizes. Since r=32 worked best, we keep this fixed for the remaining experiments.

**RQ2:** Do we benefit from more expressive circuit architectures for longer sequences?

We now consider more expressive circuits, such as MTPC-HMM and MTPC-BTREE, and show that they outperform MTPC-CP for longer MTP windows, highlighting the importance of our extension to general PCs. We fix r=32 and explore the different PC architectures for both n=8 and the longer window, n=16. Table 2 shows that MTPC-HMM obtains the best  $\mu_{\rm acc}$  in both cases, however, it strikes an unfavourable balance in the expressiveness–latency trade-off: Due to being AR, MTPC-HMM has the largest  $\mu_{lat}$ , and yields poor throughput as a result. On the other hand, MTPC-BTREE almost matches the  $\mu_{\rm acc}$  of MTPC-HMM and has a smaller  $\mu_{\rm lat}$  footprint. Nevertheless, for n=8, MTPC-CP still obtains the best  $\mu_{\rm tok/s}$ . However, when we move to n=16, MTPC-BTREE substantially increases the gap in  $\mu_{\rm acc}$  from MTPC-CP. This in turn leads to MTPC-BTREE having the best throughput, with 203.5 tok/s, a speed-up of  $\times 5.08$  over EvaByte-STP. While the gains already obtained by MTPC-BTREE are solid, fine-tuning the output layer alone can only get us so far. This is because EvaByte has not been trained to produce representations that are good for predicting 16 tokens ahead, as we discuss next.

n	model	# LoRA	$\mu_{ m acc}$ $\uparrow$	$\mu_{\mathrm{lat}}\downarrow$	$\mu_{ ext{tok/s}} \uparrow$	speed-up ↑
1	EvaByte-STP	0	_	0.0251	40.03	1.00
		0	$5.15 \pm 0.04$	$0.0327 \pm 0.0013$	$163.7 \pm 10.5$	4.09
	MmDC EE	1	$5.16 \pm 0.02$	$0.0308 \pm 0.0003$	$171.3 \pm 1.2$	4.28
	MTPC-FF	2	$5.14 \pm 0.06$	$0.0336\pm 0.0036$	$157.2 \pm 17.4$	3.93
8		4	$5.19 \pm 0.03$	$0.0330\pm 0.0001$	$160.3 \pm \text{1.4}$	4.01
	MTPC-BTree	0	$6.04 \pm 0.02$	$0.0326 \pm 0.0027$	$190.5 \pm 14.8$	4.76
		1	$6.15 \pm 0.02$	$0.0344 \pm 0.0038$	$185.1 \pm 20.3$	4.62
		2	$6.20 \pm 0.05$	$0.0330 \pm 0.0000$	$193.0 \pm 1.4$	4.82
		4	$\textbf{6.20} \pm 0.04$	$0.0348\pm {\scriptstyle 0.0001}$	$183.1 \pm \text{1.0}$	4.57
	MTPC-FF	0	$5.40 \pm 0.06$	<b>0.0305</b> ± 0.0001	$180.3 \pm 2.3$	4.50
		1	$5.53 \pm 0.08$	$0.0311 \pm 0.0001$	$182.3 \pm 2.5$	4.55
		2	$5.63 \pm 0.07$	$0.0321 \pm 0.0002$	$179.5 \pm 2.0$	4.48
16		4	$5.60 \pm 0.03$	$0.0356\pm 0.0034$	$162.2 \pm 14.9$	4.05
		0	$6.86 \pm 0.03$	$0.0340 \pm 0.0001$	$206.1 \pm 0.9$	5.15
	MTPC-BTree	1	$7.32 \pm 0.03$	$0.0346 \pm 0.0000$	$218.0 \pm 0.6$	5.45
	WITEC-BIFEE	2	$7.53\pm0.10$	$0.0354 \pm 0.0001$	$219.1 \pm 3.0$	5.47
		4	$\textbf{7.58} \pm 0.14$	$0.0373\pm 0.0003$	$210.2 \pm 5.0$	5.25

Table 3: **Fine-tuning sep**arate layers in the draft model with LoRA adapters can increase the acceptance rate and speed up BTree **MTPCs** for n = 16 and two LoRA layers by 5.47 over STP on an L40s GPU. Nevertheless, the increased acceptance rate comes at increased latency, making further throughput boosts via more LoRA layers unviable for EvaByte. We shade the STP baseline in gray and ablated models trained for the additional epoch without LoRA in brown.

TAKEAWAY 1: While increasing the mixture components r in CP is initially beneficial, it soon hits diminishing returns. Increasing the window size of future tokens n and adopting more expressive PC architectures unlocks further gains in throughput. Furthermore, while HMM achieves the highest acceptance rates, it incurs high latency. Instead, non-autoregressive variants such as BTREE strike a better balance and hence should be preferred.

#### 4.4 MTPCs WITH ADAPTERS

**RQ3:** Can we further increase throughput by adapting the draft LLM using LoRA?

We now consider increasing the expressiveness by adding LoRA layers, as shown in Table 3. We show that while we can improve throughput, we need to be strategic when choosing the number of layers, as very quickly the latency introduced outweighs the expressiveness gained.

The key here is that we need to balance the expressiveness obtained by adding LoRA layers and the latency we introduce because the additional layers are not shared between the draft and the verifier. For example, if we train adapters for the last 16 (out of 32) layers, we can improve the acceptance rate by 37%, but we introduce a latency of  $1.5\times$  the cost of a forward pass of the LLM. The FF model for n=8 has plateaued, highlighting its limited expressiveness. We highlight that the improvements of MTPC are consistent across GPUs. While throughput is  $\approx \times 2$  times larger for the server-grade GPU, the relative speed-ups are similar, see Section D. Interestingly, due to the different balance between the LLM and MTPC latency across GPUs, on the RTX 3090 we hit diminishing returns after adding a single LoRA layer rather than two on the L40s.

TAKEAWAY 2: Fine-tuning a few layers of the draft model with LoRA increases the acceptance rate but also increases latency. The optimal trade-off is device-specific, but adding LoRAs is always beneficial compared with a fully shared LLM trunk. Retrofitting models to longer MTP windows yields an even larger increase in throughput when paired with LoRAs.

# 5 Conclusion

Overall, our results show, for the first time, that throughput in MTP LLMs can be increased by  $5.47 \times$  w.r.t. AR and  $1.22 \times$  w.r.t. MTP with independence assumptions, while simultaneously guaranteeing the retention of an AR LLM's quality. We achieved this goal by identifying key trade-offs between acceptance rates and latency within our framework, MTPC. We enhanced the *expressiveness* of

<sup>&</sup>lt;sup>8</sup>We found that training more than 16 layers of EvaByte does not lead to improvements in acceptance rates.

MTP by getting rid of the independence assumption (Gloeckle et al., 2024; Zheng et al., 2025), introducing an explicit probabilistic model for inter-token dependencies that facilitates performance guarantees (Ankner et al., 2024; Li et al., 2024; DeepSeek-AI et al., 2024), and generalising mixture-based methods (Basharin et al., 2025) into the PC framework. Moreover, we decreased latency by modulating the number of layers shared between draft and verifier model branches. We showcase the throughput gains of MTPC LLMs *at scale* by retrofitting EvaByte (Zheng et al., 2025), a state-of-the-art 6.5B byte-level LLM into our framework. In future work, our framework can be extended by integrating constraints during generation via methods such as Gelato (Zhang et al., 2023) and Ctrl-G (Zhang et al., 2024a). Unlike those, we would not need to train an auxiliary HMM in MTPCs and we can integrate constraints directly into our PC head. Moreover, we can further boost expressiveness by leveraging other PCs architectures such as subtractive mixtures (Loconte et al., 2024; 2025b) and continuous latent variable circuits (Gala et al., 2024a;b), while reducing latency through recent advancements in scaling up PCs (Liu et al., 2024; Zhang et al., 2025).

#### **AUTHOR CONTRIBUTIONS**

AV, AG and LL conceived the initial idea and later discussed it with the other co-authors. AG was responsible for trading off expressivity and efficiency by limiting the number of LoRA layers and adapting speculative decoding for the self-speculative scenario. LL was responsible for the speculative decoding implementation and the development of circuits (CP, HMM, BTree). AG and LL were responsible for designing and coding models and experiments and trained the models with help from EvK, who also helped with training infrastructure. YZ and PN provided useful feedback and helped with preliminary experiments. EW provided funding and useful feedback. PM provided evaluations, guidance and useful feedback. EP helped design the experimental setup, including the choice of models and data. AG, AV and EP wrote the paper with help from LL and EvK. AV and EP supervised all phases of the project.

#### **ACKNOWLEDGEMENTS**

We would like to thank the members of april lab and Ponti lab for useful feedback during early presentations of this work.

AG was funded by NatWest Group. EvK was funded by the ELIAI project "Gradient-based Learning of Complex Latent Structures". EP was funded by the ERC Starting Grant AToM-FM (101222956). AG and AV were funded by the "UNREAL: Unified Reasoning Layer for Trustworthy ML" project (EP/Y023838/1) selected by the ERC and funded by UKRI EPSRC.

#### REPRODUCIBILITY STATEMENT

To ensure reproducibility for our research, we have attached the codebase for implementing all model variants and running their training and evaluation to our submission. In addition, we have provided full details on sampling in circuits in Section B and on our algorithms for speculative decoding in Section C.

#### REFERENCES

Orevaoghene Ahia, Sachin Kumar, Hila Gonen, Jungo Kasai, David Mortensen, Noah Smith, and Yulia Tsvetkov. Do all languages cost the same? tokenization in the era of commercial language models. In Houda Bouamor, Juan Pino, and Kalika Bali (eds.), *Proceedings of the 2023 Conference on Empirical Methods in Natural Language Processing*, pp. 9904–9923, Singapore, December 2023. Association for Computational Linguistics. doi: 10.18653/v1/2023.emnlp-main.614. URL https://aclanthology.org/2023.emnlp-main.614.

Zachary Ankner, Rishab Parthasarathy, Aniruddha Nrusimha, Christopher Rinard, Jonathan Ragan-Kelley, and William Brandon. Hydra: Sequentially-dependent draft heads for medusa decoding. In *First Conference on Language Modeling*, 2024. URL https://openreview.net/forum?id=FbhjirzvJG.

<sup>&</sup>lt;sup>9</sup>More in-depth commentary on related work is available in Section H.

- Artem Basharin, Andrei Chertkov, and Ivan Oseledets. Faster language models with better multi-token prediction using tensor decomposition. *arXiv* preprint arXiv:2410.17765, 2025.
- Tianle Cai, Yuhong Li, Zhengyang Geng, Hongwu Peng, Jason D. Lee, Deming Chen, and Tri Dao. Medusa: Simple llm inference acceleration framework with multiple decoding heads. *arXiv* preprint arXiv: 2401.10774, 2024.
- Charlie Chen, Sebastian Borgeaud, Geoffrey Irving, Jean-Baptiste Lespiau, L. Sifre, and John M. Jumper. Accelerating large language model decoding with speculative sampling. *ArXiv*, abs/2302.01318, 2023.
- Song Cheng, Lei Wang, Tao Xiang, and Pan Zhang. Tree tensor networks for generative modeling. *Physical Review B*, 99(15):155131, 2019.
- YooJung Choi, Antonio Vergari, and Guy Van den Broeck. Probabilistic circuits: A unifying framework for tractable probabilistic modeling. Technical report, University of California, Los Angeles (UCLA), 2020.
- Gautier Dagan, Gabriel Synnaeve, and Baptiste Rozière. Getting the most out of your tokenizer for pre-training and domain adaptation, 2024.
- Adnan Darwiche. A differential approach to inference in bayesian networks. *Journal of the ACM (JACM)*, 50:280–305, 2003.
- Adnan Darwiche. *Modeling and Reasoning with Bayesian Networks*. Cambridge University Press, 2009.
- Adnan Darwiche and Pierre Marquis. A knowledge compilation map. *Journal of Artificial Intelligence Research (JAIR)*, 17:229–264, 2002.
- DeepSeek-AI, Aixin Liu, Bei Feng, Bing Xue, Bingxuan Wang, Bochao Wu, Chengda Lu, Chenggang Zhao, Chengqi Deng, Chenyu Zhang, Chong Ruan, Damai Dai, Daya Guo, Dejian Yang, Deli Chen, Dongjie Ji, Erhang Li, Fangyun Lin, Fucong Dai, Fuli Luo, Guangbo Hao, Guanting Chen, Guowei Li, H. Zhang, Han Bao, Hanwei Xu, Haocheng Wang, Haowei Zhang, Honghui Ding, Huajian Xin, Huazuo Gao, Hui Li, Hui Qu, J. L. Cai, Jian Liang, Jianzhong Guo, Jiaqi Ni, Jiashi Li, Jiawei Wang, Jin Chen, Jingchang Chen, Jingyang Yuan, Junjie Qiu, Junlong Li, Junxiao Song, Kai Dong, Kai Hu, Kaige Gao, Kang Guan, Kexin Huang, Kuai Yu, Lean Wang, Lecong Zhang, Lei Xu, Leyi Xia, Liang Zhao, Litong Wang, Liyue Zhang, Meng Li, Miaojun Wang, Mingchuan Zhang, Minghua Zhang, Minghui Tang, Mingming Li, Ning Tian, Panpan Huang, Peiyi Wang, Peng Zhang, Qiancheng Wang, Qihao Zhu, Qinyu Chen, Qiushi Du, R. J. Chen, R. L. Jin, Ruiqi Ge, Ruisong Zhang, Ruizhe Pan, Runji Wang, Runxin Xu, Ruoyu Zhang, Ruyi Chen, S. S. Li, Shanghao Lu, Shangyan Zhou, Shanhuang Chen, Shaoqing Wu, Shengfeng Ye, Shengfeng Ye, Shirong Ma, Shiyu Wang, Shuang Zhou, Shuiping Yu, Shunfeng Zhou, Shuting Pan, T. Wang, Tao Yun, Tian Pei, Tianyu Sun, W. L. Xiao, Wangding Zeng, Wanjia Zhao, Wei An, Wen Liu, Wenfeng Liang, Wenjun Gao, Wenqin Yu, Wentao Zhang, X. Q. Li, Xiangyue Jin, Xianzu Wang, Xiao Bi, Xiaodong Liu, Xiaohan Wang, Xiaojin Shen, Xiaokang Chen, Xiaokang Zhang, Xiaosha Chen, Xiaotao Nie, Xiaowen Sun, Xiaoxiang Wang, Xin Cheng, Xin Liu, Xin Xie, Xingchao Liu, Xingkai Yu, Xinnan Song, Xinxia Shan, Xinyi Zhou, Xinyu Yang, Xinyuan Li, Xuecheng Su, Xuheng Lin, Y. K. Li, Y. Q. Wang, Y. X. Wei, Y. X. Zhu, Yang Zhang, Yanhong Xu, Yanhong Xu, Yanping Huang, Yao Li, Yao Zhao, Yaofeng Sun, Yaohui Li, Yaohui Wang, Yi Yu, Yi Zheng, Yichao Zhang, Yifan Shi, Yiliang Xiong, Ying He, Ying Tang, Yishi Piao, Yisong Wang, Yixuan Tan, Yiyang Ma, Yiyuan Liu, Yongqiang Guo, Yu Wu, Yuan Ou, Yuchen Zhu, Yuduan Wang, Yue Gong, Yuheng Zou, Yujia He, Yukun Zha, Yunfan Xiong, Yunxian Ma, Yuting Yan, Yuxiang Luo, Yuxiang You, Yuxuan Liu, Yuyang Zhou, Z. F. Wu, Z. Z. Ren, Zehui Ren, Zhangli Sha, Zhe Fu, Zhean Xu, Zhen Huang, Zhen Zhang, Zhenda Xie, Zhengyan Zhang, Zhewen Hao, Zhibin Gou, Zhicheng Ma, Zhigang Yan, Zhihong Shao, Zhipeng Xu, Zhiyu Wu, Zhongyu Zhang, Zhuoshu Li, Zihui Gu, Zijia Zhu, Zijun Liu, Zilin Li, Ziwei Xie, Ziyang Song, Ziyi Gao, and Zizheng Pan. Deepseek-v3 technical report, 2024. URL https://arxiv.org/abs/2412.19437.

Gennaro Gala, Cassio de Campos, Robert Peharz, Antonio Vergari, and Erik Quaeghebeur. Probabilistic integral circuits. In *AISTATS 2024*, 2024a.

- Gennaro Gala, Cassio de Campos, Antonio Vergari, and Erik Quaeghebeur. Scaling continuous latent variable models as probabilistic integral circuits. *arXiv preprint arXiv:2406.06494*, 2024b.
- Jonas Geiping, Alex Stein, Manli Shu, Khalid Saifullah, Yuxin Wen, and Tom Goldstein. Coercing LLMs to do and reveal (almost) anything. In *ICLR 2024 Workshop on Secure and Trustworthy Large Language Models*, 2024. URL https://openreview.net/forum?id=Y5inHAjMu0.
- Fabian Gloeckle, Badr Youbi Idrissi, Baptiste Rozière, David Lopez-Paz, and Gabriel Synnaeve. Better & faster large language models via multi-token prediction. *arXiv preprint arXiv:2404.19737*, 2024.
- Lars Grasedyck. Hierarchical singular value decomposition of tensors. SIAM journal on matrix analysis and applications, 31(4):2029–2054, 2010.
- Edward J Hu, yelong shen, Phillip Wallis, Zeyuan Allen-Zhu, Yuanzhi Li, Shean Wang, Lu Wang, and Weizhu Chen. LoRA: Low-rank adaptation of large language models. In *International Conference on Learning Representations*, 2022. URL https://openreview.net/forum?id=nZeVKeeFYf9.
- Siming Huang, Tianhao Cheng, Jason Klein Liu, Jiaran Hao, Liuyihan Song, Yang Xu, J. Yang, J. H. Liu, Chenchen Zhang, Linzheng Chai, Ruifeng Yuan, Zhaoxiang Zhang, Jie Fu, Qian Liu, Ge Zhang, Zili Wang, Yuan Qi, Yinghui Xu, and Wei Chu. Opencoder: The open cookbook for top-tier code large language models. 2024. URL https://arxiv.org/pdf/2411.04905.
- Yoon Kim and Alexander M. Rush. Sequence-level knowledge distillation. In Jian Su, Kevin Duh, and Xavier Carreras (eds.), *Proceedings of the 2016 Conference on Empirical Methods in Natural Language Processing*, pp. 1317–1327, Austin, Texas, November 2016. Association for Computational Linguistics. doi: 10.18653/v1/D16-1139. URL https://aclanthology.org/D16-1139/.
- Diederik P. Kingma and Jimmy Ba. Adam: A method for stochastic optimization. In *3rd International Conference on Learning Representations (ICLR)*, 2015.
- Tamara G Kolda and Brett W Bader. Tensor decompositions and applications. *SIAM review*, 51(3): 455–500, 2009.
- Nathan Lambert, Jacob Morrison, Valentina Pyatkin, Shengyi Huang, Hamish Ivison, Faeze Brahman, Lester James V. Miranda, Alisa Liu, Nouha Dziri, Shane Lyu, Yuling Gu, Saumya Malik, Victoria Graf, Jena D. Hwang, Jiangjiang Yang, Ronan Le Bras, Oyvind Tafjord, Chris Wilhelm, Luca Soldaini, Noah A. Smith, Yizhong Wang, Pradeep Dasigi, and Hannaneh Hajishirzi. Tülu 3: Pushing frontiers in open language model post-training. 2024.
- Adrian Łańcucki, Konrad Staniszewski, Piotr Nawrot, and Edoardo M Ponti. Inference-time hyperscaling with KV cache compression, 2025.
- Sander Land and Max Bartolo. Fishing for magikarp: Automatically detecting under-trained tokens in large language models, 2024.
- Jason Lee, Elman Mansimov, and Kyunghyun Cho. Deterministic non-autoregressive neural sequence modeling by iterative refinement. In Ellen Riloff, David Chiang, Julia Hockenmaier, and Jun'ichi Tsujii (eds.), *Proceedings of the 2018 Conference on Empirical Methods in Natural Language Processing*, pp. 1173–1182, Brussels, Belgium, October-November 2018. Association for Computational Linguistics. doi: 10.18653/v1/D18-1149. URL https://aclanthology.org/D18-1149/.
- Yaniv Leviathan, Matan Kalman, and Yossi Matias. Fast inference from transformers via speculative decoding. In *International Conference on Machine Learning (ICML)*, 2022.
- Yuhui Li, Fangyun Wei, Chao Zhang, and Hongyang Zhang. Eagle: speculative sampling requires rethinking feature uncertainty. In *Proceedings of the 41st International Conference on Machine Learning*, ICML'24. JMLR.org, 2024.
- Anji Liu, Kareem Ahmed, and Guy Van den Broeck. Scaling tractable probabilistic circuits: A systems perspective. *arXiv* preprint arXiv:2406.00766, 2024.

- Lorenzo Loconte, M. Sladek Aleksanteri, Stefan Mengel, Martin Trapp, Arno Solin, Nicolas Gillis, and Antonio Vergari. Subtractive mixture models via squaring: Representation and learning. In *The Twelfth International Conference on Learning Representations (ICLR)*, 2024.
- Lorenzo Loconte, Antonio Mari, Gennaro Gala, Robert Peharz, Cassio de Campos, Erik Quaeghebeur, Gennaro Vessio, and Antonio Vergari. What is the Relationship between Tensor Factorizations and Circuits (and How Can We Exploit it)? *Transactions on Machine Learning Research*, 2025a. ISSN 2835-8856. Featured Certification.
- Lorenzo Loconte, Stefan Mengel, and Antonio Vergari. Sum of Squares Circuits. In *The 39th Annual AAAI Conference on Artificial Intelligence (AAAI)*, 2025b.
- Antonio Mari, Gennaro Vessio, and Antonio Vergari. Unifying and understanding overparameterized circuit representations via low-rank tensor decompositions. In *6th Workshop on Tractable Probabilistic Modeling*, 2023.
- Benjamin Minixhofer, Ivan Vulić, and Edoardo Maria Ponti. Cross-tokenizer distillation via approximate likelihood matching, 2025. URL https://arxiv.org/abs/2503.20083.
- Piotr Nawrot, Jan Chorowski, Adrian Lancucki, and Edoardo Maria Ponti. Efficient transformers with dynamic token pooling. In Anna Rogers, Jordan Boyd-Graber, and Naoaki Okazaki (eds.), *Proceedings of the 61st Annual Meeting of the Association for Computational Linguistics (Volume 1: Long Papers)*, pp. 6403–6417, Toronto, Canada, July 2023. Association for Computational Linguistics. doi: 10.18653/v1/2023.acl-long.353. URL https://aclanthology.org/2023.acl-long.353.
- Piotr Nawrot, Adrian Łańcucki, Marcin Chochowski, David Tarjan, and Edoardo Ponti. Dynamic memory compression: Retrofitting LLMs for accelerated inference. In *Forty-first International Conference on Machine Learning*, 2024. URL https://openreview.net/forum?id=tdryrAkob7.
- Artidoro Pagnoni, Ram Pasunuru, Pedro Rodriguez, John Nguyen, Benjamin Muller, Margaret Li, Chunting Zhou, Lili Yu, Jason Weston, Luke Zettlemoyer, Gargi Ghosh, Mike Lewis, Ari Holtzman, and Srinivasan Iyer. Byte latent transformer: Patches scale better than tokens, 2024. URL https://arxiv.org/abs/2412.09871.
- Robert Peharz, Sebastian Tschiatschek, Franz Pernkopf, and Pedro M. Domingos. On Theoretical Properties of Sum-Product Networks. In *International Conference on Artificial Intelligence and Statistics*, 2015.
- Robert Peharz, Steven Lang, Antonio Vergari, Karl Stelzner, Alejandro Molina, Martin Trapp, Guy Van den Broeck, Kristian Kersting, and Zoubin Ghahramani. Einsum networks: Fast and scalable learning of tractable probabilistic circuits. In *International Conference on Machine Learning*, pp. 7563–7574. PMLR, 2020a.
- Robert Peharz, Antonio Vergari, Karl Stelzner, Alejandro Molina, Xiaoting Shao, Martin Trapp, Kristian Kersting, and Zoubin Ghahramani. Random sum-product networks: A simple and effective approach to probabilistic deep learning. In 35th Conference on Uncertainty in Artificial Intelligence (UAI), volume 115 of Proceedings of Machine Learning Research, pp. 334–344. PMLR, 2020b.
- Jessica Rumbelow and Matthew Watkins. Solidgoldmagikarp (plus, prompt generation), 2023. https://www.lesswrong.com/posts/aPeJE8bSo6rAFoLqg/solidgoldmagikarp-plus-prompt-generation.
- Elizabeth Salesky, David Etter, and Matt Post. Robust open-vocabulary translation from visual text representations. In Marie-Francine Moens, Xuanjing Huang, Lucia Specia, and Scott Wen-tau Yih (eds.), *Proceedings of the 2021 Conference on Empirical Methods in Natural Language Processing*, pp. 7235–7252, Online and Punta Cana, Dominican Republic, November 2021. Association for Computational Linguistics. doi: 10.18653/v1/2021.emnlp-main.576. URL https://aclanthology.org/2021.emnlp-main.576.

- Xiaoting Shao, Alejandro Molina, Antonio Vergari, Karl Stelzner, Robert Peharz, Thomas Liebig, and Kristian Kersting. Conditional sum-product networks: Imposing structure on deep probabilistic architectures. In *International Conference on Probabilistic Graphical Models*, pp. 401–412. PMLR, 2020.
- Xiaoting Shao, Alejandro Molina, Antonio Vergari, Karl Stelzner, Robert Peharz, Thomas Liebig, and Kristian Kersting. Conditional sum-product networks: Modular probabilistic circuits via gate functions. *International Journal of Approximate Reasoning*, 140:298–313, 2022.
- Amir Shpilka and Amir Yehudayoff. Arithmetic circuits: A survey of recent results and open questions. *Foundations and Trends in Theoretical Computer Science*, 5:207–388, 2010.
- Mitchell Stern, Noam M. Shazeer, and Jakob Uszkoreit. Blockwise parallel decoding for deep autoregressive models. In *Neural Information Processing Systems (NeurIPS)*, 2018.
- Ziteng Sun, Ananda Theertha Suresh, Jae Hun Ro, Ahmad Beirami, Himanshu Jain, and Felix Yu. Spectr: Fast speculative decoding via optimal transport. In *Thirty-seventh Conference on Neural Information Processing Systems*, 2023. URL https://openreview.net/forum?id=SdYHLTCC5J.
- The april Lab. cirkit, October 2024. URL https://github.com/april-tools/cirkit.
- Cristiano Varin, Nancy Reid, and David Firth. An overview of composite likelihood methods. *Statistica Sinica*, 21, 01 2011.
- Antonio Vergari, Nicola Di Mauro, and Floriana Esposito. Visualizing and understanding sum-product networks. *Machine Learning*, 108(4):551–573, 2019a.
- Antonio Vergari, Nicola Di Mauro, and Guy Van den Broeck. Tractable probabilistic models: Representations, algorithms, learning, and applications. *Tutorial at the 35th Conference on Uncertainty in Artificial Intelligence (UAI)*, 2019b.
- Antonio Vergari, YooJung Choi, Anji Liu, Stefano Teso, and Guy Van den Broeck. A compositional atlas of tractable circuit operations for probabilistic inference. In *Advances in Neural Information Processing Systems 34 (NeurIPS)*, pp. 13189–13201. Curran Associates, Inc., 2021.
- Junxiong Wang, Tushaar Gangavarapu, Jing Nathan Yan, and Alexander M. Rush. Mambabyte: Token-free selective state space model, 2024. URL https://arxiv.org/abs/2401.13660.
- Davis Wertheimer, Joshua Rosenkranz, Thomas Parnell, Sahil Suneja, Pavithra Ranganathan, Raghu Ganti, and Mudhakar Srivatsa. Accelerating production llms with combined token/embedding speculators, 2024. URL https://arxiv.org/abs/2404.19124.
- Heming Xia, Zhe Yang, Qingxiu Dong, Peiyi Wang, Yongqi Li, Tao Ge, Tianyu Liu, Wenjie Li, and Zhifang Sui. Unlocking efficiency in large language model inference: A comprehensive survey of speculative decoding. In Lun-Wei Ku, Andre Martins, and Vivek Srikumar (eds.), *Findings of the Association for Computational Linguistics ACL 2024*, pp. 7655–7671, Bangkok, Thailand and virtual meeting, August 2024. Association for Computational Linguistics. doi: 10.18653/v1/2024. findings-acl.456. URL https://aclanthology.org/2024.findings-acl.456.
- Lili Yu, Daniel Simig, Colin Flaherty, Armen Aghajanyan, Luke Zettlemoyer, and Mike Lewis. Megabyte: Predicting million-byte sequences with multiscale transformers. In A. Oh, T. Naumann, A. Globerson, K. Saenko, M. Hardt, and S. Levine (eds.), Advances in Neural Information Processing Systems, volume 36, pp. 78808–78823. Curran Associates, Inc., 2023. URL https://proceedings.neurips.cc/paper\_files/paper/2023/file/f8f78f8043f35890181a824e53a57134-Paper-Conference.pdf.
- Honghua Zhang, Meihua Dang, Nanyun Peng, and Guy Van Den Broeck. Tractable control for autoregressive language generation. In Andreas Krause, Emma Brunskill, Kyunghyun Cho, Barbara Engelhardt, Sivan Sabato, and Jonathan Scarlett (eds.), *Proceedings of the 40th International Conference on Machine Learning*, volume 202 of *Proceedings of Machine Learning Research*, pp. 40932–40945. PMLR, 23–29 Jul 2023. URL https://proceedings.mlr.press/v202/zhang23g.html.

- Honghua Zhang, Po-Nien Kung, Masahiro Yoshida, Guy Van den Broeck, and Nanyun Peng. Adaptable logical control for large language models. In A. Globerson, L. Mackey, D. Belgrave, A. Fan, U. Paquet, J. Tomczak, and C. Zhang (eds.), *Advances in Neural Information Processing Systems*, volume 37, pp. 115563–115587. Curran Associates, Inc., 2024a. URL https://proceedings.neurips.cc/paper\_files/paper/2024/file/d15c16cf5619a2b1606da5fc88e3fla9-Paper-Conference.pdf.
- Honghua Zhang, Meihua Dang, Benjie Wang, Stefano Ermon, Nanyun Peng, and Guy Van den Broeck. Scaling probabilistic circuits via monarch matrices. arXiv preprint arXiv:2506.12383, 2025.
- Jun Zhang, Jue Wang, Huan Li, Lidan Shou, Ke Chen, Gang Chen, and Sharad Mehrotra. Draft & verify: Lossless large language model acceleration via self-speculative decoding. In Lun-Wei Ku, Andre Martins, and Vivek Srikumar (eds.), *Proceedings of the 62nd Annual Meeting of the Association for Computational Linguistics (Volume 1: Long Papers)*, pp. 11263–11282, Bangkok, Thailand, August 2024b. Association for Computational Linguistics. doi: 10.18653/v1/2024. acl-long.607. URL https://aclanthology.org/2024.acl-long.607/.
- Lin Zheng, Xueliang Zhao, Guangtao Wang, Chen Wu, David Dong, Angela Wang, Mingran Wang, Yun Du, Haige Bo, Amol Sharma, Bo Li, Kejie Zhang, Changran Hu, Urmish Thakker, and Lingpeng Kong. Evabyte: Efficient byte-level language models at scale, 2025. URL https://hkunlp.github.io/blog/2025/evabyte.

# A NOTATION

We adapt notation and nomenclature from the tensor factorisation (Kolda & Bader, 2009) and circuit (Loconte et al., 2025a) literature.

We denote ordered sets of random variables with  $\mathbf{X}$ ,  $\mathbf{Y}$  and  $\mathbf{Z}$ , and we use [n] to express the set  $\{1,2,\ldots,n\}$  with n>0. The domain of a variable X is denoted as  $\mathrm{dom}(X)$ , and we denoted as  $\mathrm{dom}(\mathbf{X})=\mathrm{dom}(X_1)\times\cdots\times\mathrm{dom}(X_n)$  the joint domain of variables  $\mathbf{X}=\{X_i\}_{i=1}^n$ . We denote scalars with lower-case letters (e.g.,  $a\in\mathbb{R}$ ), vectors with boldface lower-case letters (e.g.,  $\mathbf{a}\in\mathbb{R}^N$ ), matrices with boldface upper-case letters (excluding those used for variables, e.g.,  $\mathbf{A}\in\mathbb{R}^{M\times N}$ ), and tensors with boldface calligraphic letters (e.g.,  $\mathbf{A}\in\mathbb{R}^{I_1\times I_2\times I_3}$ ). Moreover, we use subscripts to denote entries of tensors (e.g.,  $a_{ijk}$  is the (i,j,k)-th entry in  $\mathbf{A}$ ).

# B BACKGROUND ON CIRCUITS

Circuits have a long history in theoretical computer science (Shpilka & Yehudayoff, 2010) and probabilistic reasoning (Darwiche, 2003; 2009). In their more modern definition and application to machine learning (Vergari et al., 2019b; Choi et al., 2020), circuits are introduced as structured computational graphs, simplified neural networks where one is allowed to use units from a restricted set of neurons (sum, product and input units) and whose connections need to abide certain *structural* properties to guarantee tractability (Choi et al., 2020; Vergari et al., 2021), as discussed next.

#### **B.1** STRUCTURAL PROPERTIES

Tractability is to be intended as the ability to exactly compute a given function (operation) over the circuit in time that is polynomial in its size, denoted as |c| for a circuit c, and representing the number of edges between the computational units. For example, a circuit c can exactly integrate *any subset of variables* in time  $\mathcal{O}(|c|)$  if (i) its input functions can be integrated efficiently and (ii) it is *smooth* and *decomposable* (Darwiche & Marquis, 2002; Choi et al., 2020).

**Definition 1** (Smoothness and decomposability (Darwiche & Marquis, 2002; Choi et al., 2020)). A circuit is *smooth* if for every sum unit n, all its input units depend on the same variables, i.e.,  $\forall i, j \in \text{in}(n) : \text{sc}(i) = \text{sc}(j)$ . A circuit is *decomposable* if the distinct inputs of every product unit n depend on disjoint sets of variables, i.e.,  $\forall i, j \in \text{in}(n) \ i \neq j : \text{sc}(i) \cap \text{sc}(j) = \emptyset$ .

Note that all the PC architectures we have discussed in this paper, FF, CP, HMM and BTree, are smooth and decomposable circuits. The reader is encouraged to check this by themselves for the architectures in Fig. 2.

Exactly integrating variables out is relevant to compute marginals such as the normalisation constant of the distribution encoded by the circuit (Eq. (3)). Note that in our implementation, circuits are normalised by design (Peharz et al., 2015), as we assume that input distributions are normalised categoricals and all sum units form a convex combination as their weights are parameterised with a softmax function (see Section 3.3).

More importantly for our MTPCs, we can draw samples efficiently from the distribution of a circuit that is both smooth and decomposable, as we discuss in the next sub-section.

#### B.2 SAMPLING A CIRCUIT

A smooth and decomposable PC can use ancestral sampling to generate a complete sample for all n tokens in a window. In a nutshell, we can iteratively sample each latent variable in the hierarchy encoded by the PC, and then sample the selected input distributions, in the same way one sample one (hierarchical) mixture model by first sampling one component and then drawing a sample from that component.

Operationally, Algorithm 1 details the procedure. We have to sample one input branch for each sum unit we encounter when performing a backward traversal of the circuit computational graph (from the circuit output back to the input distributions). Such a branch is sampled proportionally to the sum unit weights  $\omega_j$ , which encode the mixture components (or equivalently the transition probabilities in

# **Algorithm 1** SAMPLE(c)

**Input:** A smooth, decomposable and normalised PC c encoding a joint distribution q over the next n tokens  $\mathbf{X} = \{X_1, \dots, X_n\}$  **Output:** a sample  $\mathbf{x} \sim q(\mathbf{X})$ .

```
1: \mathbf{x} \leftarrow \mathsf{zeroes}(n)
                                                                                                                                    ⊳ init empty sample
 2: c_n \leftarrow \mathsf{output}(c)
 3: \mathcal{N} \leftarrow \mathsf{queue}(\{c_n\})
                                                                     ▶ traverse the computational graph from outputs to inputs
 4: while \mathcal{N} not empty do
            c_n \leftarrow \mathsf{pop}(\hat{\mathcal{N}})
if c_n = \sum_{j=1}^r \omega_j c_j then
 5:
                                                                                                                                        \triangleright c_n is a sum unit
 6:
                  k \leftarrow \mathsf{sampleCategorical}(\omega_1, \dots, \omega_r)
                                                                                    \triangleright sample from a categorical with r states
 7:
            \mathcal{N} \leftarrow \mathsf{push}(\mathcal{N}, c_k)

else if c_n = \prod_{j=1}^d c_j then

for k = 1 \dots d do
 8:
 9:
                                                                                                           \triangleright c_n is a product unit with d inputs
10:
                         \mathcal{N} \leftarrow \mathsf{push}(\mathcal{N}, c_k)
                                                                                                                                 \triangleright visit all inputs of c_n
11:
            else if c_n is an input unit over variable X_i and parameters \phi_i then
12:
                   x_i \leftarrow \mathsf{sampleCategorical}(\phi_i)
                                                                                     \triangleright sample from a categorical with v = |\mathcal{V}| states
13:
14: return x
```

an HMM). Then, when we traverse a product unit, we follow all its input branches. When we reach an input unit, we sample a token proportionally to the parameters  $\phi_{ij}$  of the categorical distributions encoded in the unit.

If the circuit is smooth and decomposable, by this process we are guaranteed to end up in a set of input units whose scope is the full set of tokens X and in which only one input unit is selected per token position i (line 13 of Algorithm 1). This procedure can be tensorized as to efficiently generate a batch of samples in a single pass over the computational graph of the circuit (Vergari et al., 2019a; Peharz et al., 2020b;a; Loconte et al., 2025a; Liu et al., 2024).

Lastly, we remark that this routine is potentially computationally more efficient than the one implemented in Basharin et al. (2025), as the latter is based on autoregressive inverse transform sampling (see Loconte et al. (2024) for a discussion) and requires sampling one token at a time.

## C SPECULATIVE DECODING

We give pseudocode for our self-speculative decoding algorithm below. The algorithm accepts between 0 and n tokens, but always generates between 1 and n tokens, where n is the MTP window size. The algorithm is very similar to vanilla speculative decoding (Leviathan et al., 2022), but our algorithm includes a modification that reduces latency for the self-speculative scenario, and for this it needs to sacrifice the last "free" token typically obtained from the verifier. The gain in latency is possible because we can evaluate the shared LLM once per draft/verify cycle, while a naive implementation of Leviathan et al. (2022) for self-speculative decoding would need two, approximately halving the possible throughput.

In our self-speculative setup, the verifier and draft LLMs share some layers of the backbone. Importantly, the verifier is always computing LLM states ahead of the draft. As such, we can get away with a single forward pass through the shared LLM, similar to Medusa (Cai et al., 2024), by re-using the LLM backbone state computed by the verifier for the draft model. For this to work, we cannot accept a "last sample for free" from the verifier (lines 23-30) Algorithm 3), as we would not have the backbone state for this new token and it is not worth paying an extra LLM evaluation for it. Therefore, in our algorithm we only sample the "free" token from the verifier in the rare case that no tokens are accepted. This is necessary because the model can get caught in successive no-accept states in the sampling case, or get stuck in an infinite loop if we used greedy decoding. If any tokens were accepted, we use the last state of the shared backbone computed during the verify phase to seed the draft phase. In what follows, if we have no LoRA layers, the algorithm is modified to have a single component: the shared encoder.

# Algorithm 2 SHAREDSTATESELFSPECULATIVEDECODING

# **Architecture Components:**

Three components: Shared Encoder (S), Verifier (V), Draft (D)

Each with their own KV-cache

**Given:** A prompt of length L

**Initialisation:** 

Prefill V to L-1, and D and S to L

Set S and D state

## Switch to draft/verify cycle:

while true do

#### **Draft stage:**

if S state is not set then

Compute S by conditioning on the additional token

Use S state to compute D state

Parameterize MTPC with D state

Draft n tokens

# Verify stage:

Compute  $\bar{S}$  state on n+1 tokens (draft + predecessor)

Compute V state using S state

Obtain up to n + 1 tokens from speculative decoding

if 0 tokens accepted then

Keep "free" token sampled from last valid logits

Unset S state (stale)

## else

Accept n tokens (drop "free" token)

Set S state (hidden state for last accepted token)

# Algorithm 3 SelfSpeculativeDecoding( $\mathbf{x}_{\leq t}, f, h, c, g$ )

**Input:** A prefix  $\mathbf{x}_{\leq t}$  of length t, an LLM backbone  $f \colon \mathcal{V}^* \to \mathbb{R}^d$ , an LLM head  $h \colon \mathbb{R}^d \to \Theta$  parameterising a PC c encoding a joint distribution q over the next n tokens, and an LLM head  $g \colon \mathbb{R}^d \to \Delta^v$  computing the next token probabilities.

**Output:** A sentence  $(\mathbf{x}_{\leq t} \mid\mid \mathbf{x}_{t+1:t+s}) \in \mathcal{V}^{t+s}$  where  $1 \leq s \leq n+1$ . Moreover, we have that  $\mathbf{x}_{t+1:t+s} \sim p(x_{t+1},\ldots,x_{t+s} \mid \mathbf{x}_{\leq t})$  as equivalently encoded by the autoregressive single token prediction model consisting of f and g only (Leviathan et al., 2022).

```
1: \mathbf{e}_t \leftarrow f(\mathbf{x}_{\leq t})
                                                                                                                  ▷ Compute the last embedding
 2: \boldsymbol{\theta} \leftarrow h(\mathbf{e}_t)
                                                                                                             3:
 4: Let q(\mathbf{X}_{t+1:t+n} \mid \mathbf{x}_{\leq t}) = \frac{1}{Z_{\boldsymbol{\theta}}} c(\mathbf{X}_{t+1:t+n} \mid \boldsymbol{\theta})
 5: \mathbf{x}_{t+1:t+n} \sim q(\mathbf{X}_{t+1:t+n} \mid \mathbf{x}_{\leq t})
                                                                                                 \triangleright Sample n tokens from c in time \mathcal{O}(|c|)
 6: \mathbf{x} \leftarrow \mathbf{x}_{\leq t} \mid\mid \mathbf{x}_{t+1:t+n}
                                                                                              \triangleright Concatenate the prefix with the n tokens
 7:
 8: Compute in parallel for 1 \le i \le n:
                                                                                                        \triangleright Compute marginals in time \mathcal{O}(|c|)
              q(\mathbf{x}_{t+1:t+i} \mid \mathbf{x}_{\leq t}) = \sum_{x_{t+i+1},\dots,x_{t+n} \in \mathcal{V}} q(\mathbf{x}_{t+1:t+n} \mid \mathbf{x}_{\leq t})
 9:
10:
11: Compute in parallel for 1 \le i \le n+1:

    Compute target model conditionals

12:
              p(X_{t+i} \mid \mathbf{x}_{\leq t+i-1}) = g(\mathbf{e}_{t+i-1}), \text{ where } \mathbf{e}_{t+i-1} = f(\mathbf{x}_{\leq t+i-1})
13:
14: s \leftarrow 0
                                                                     \triangleright Determine the number of accepted tokens s, 0 \le s \le n
15: while s < n do
            \alpha \sim \mathcal{U}(0,1)
16:
            if s > 0 then
17:
                   q(x_{t+s+1} \mid \mathbf{x}_{\leq t+s}) \leftarrow q(\mathbf{x}_{t+1:t+s+1} \mid \mathbf{x}_{\leq t})/q(\mathbf{x}_{t+1:t+s} \mid \mathbf{x}_{\leq t})
18:
19:
            if \alpha > p(x_{t+s+1} | \mathbf{x}_{t+s})/q(x_{t+s+1} | \mathbf{x}_{t+s}) then
20:
                   exit loop
21:
            s \leftarrow s + 1
22:
23:
                                                               ▷ Sample one last token from the autoregressive LLM model
24: if s < n then
                                                                        ▶ Adjust the distribution first, if we accept fewer tokens
25:
            Let s(X_{t+s+1}) = q(X_{t+s+1} \mid \mathbf{x}_{\leq t+s})
            Let m(X_{t+s+1}) = \max(0, \ p(X_{t+s+1} \mid \mathbf{x}_{\leq t+s}) - s(X_{t+s+1}))
r(X_{t+s+1} \mid \mathbf{x}_{t+s}) = m(X_{t+s+1})/Z, with Z = \sum_{x' \in \mathcal{V}} m(x')
26:
27:
28:
            x_{t+s+1} \sim r(X_{t+s+1} \mid \mathbf{x}_{\le t+s})
29: else
            x_{t+s+1} \sim p(X_{t+s+1} \mid \mathbf{x}_{\leq t+s})
30:
31: return \mathbf{x}_{\leq t+s} || x_{t+s+1}
```

# D Additional Results on an RTX 3090

circuit	r	$\mu_{ m acc}$ $\uparrow$	$\mu_{ ext{lat}}\downarrow$	$\mu_{\text{tok/s}} \uparrow$	$\max\nolimits_{tok/s}$
FF	1	$5.12 \pm 0.03$	$0.0519 \pm 0.0003$	$101.2 \pm 0.1$	167.69
	8	$5.65 \pm 0.03$	$0.0545 \pm 0.0003$	$106.3 \pm 0.4$	161.49
	16	$5.78\pm0.06$	$0.0530 \pm 0.0002$	$112.2 \pm 1.0$	159.22
CP	32	$5.84 \pm 0.04$	$0.0532 \pm 0.0004$	$113.1 \pm 0.5$	158.55
	64	$5.88 \pm 0.03$	$0.0532 \pm 0.0001$	$113.8 \pm 0.8$	155.04
	128	$5.94 \pm 0.03$	$0.0533\pm 0.0001$	$\textbf{114.8} \pm 0.4$	153.24

Table 4: Increasing the mixture components (r) increases the throughput  $(\mu_{\text{tok/s}})$  as seen for MTPC-CP (n=8) over our baseline on an RTX 3090, EvaByte-MTP (FF) (in gray) where we report the mean  $\pm$  std over three sets of 250 prompts. MTPC-CP increases throughput as it has a larger acceptance rate  $(\mu_{\text{acc}})$  and a latency  $(\mu_{\text{lat}})$  that is constant in r.

$\overline{n}$	r	model	$\mu_{ m acc}$ $\uparrow$	$\mu_{\mathrm{lat}}\downarrow$	$\mu_{ ext{tok/s}}$ $\uparrow$	speed-up ↑
1	1	STP	_	0.047	21.4	1.00
8	32	FF HMM BTREE CP	$5.97 \pm 0.05$ $5.94 \pm 0.02$	$\begin{array}{c} \textbf{0.0519} \pm 0.0003 \\ 0.0594 \pm 0.0001 \\ 0.0546 \pm 0.0005 \\ 0.0532 \pm 0.0004 \end{array}$	$103.3 \pm 1.0 \\ 111.9 \pm 1.1$	× 4.73 × 4.83 × 5.23 × <b>5.29</b>
16	•	FF HMM CP BTREE	$6.81 \pm 0.07 \\ 6.13 \pm 0.03$	$\begin{array}{c} \textbf{0.0530} \pm 0.0003 \\ 0.0701 \pm 0.0002 \\ 0.0547 \pm 0.0003 \\ 0.0578 \pm 0.0005 \end{array}$	$99.7 \pm 0.8 \\ 115.4 \pm 1.3$	× 4.87 × 4.66 × 5.39 × <b>5.56</b>

Table 5: More expressive architectures such as MTPC-BTREE outperform MTPC-CP on longer windows in terms of throughput for n=8 and n=16 for no LoRA models on an RTX 3090 GPU. We shade the baselines in gray, these are EvaByte-STP and the fully factorised (FF) models trained for the same steps as our circuits.

$\overline{n}$	model	# LoRA	$\mu_{ m acc}$ $\uparrow$	$\mu_{\mathrm{lat}}\downarrow$	$\mu_{ ext{tok/s}}$ $\uparrow$	speed-up↑
1	STP	0	_	0.047	21.40	1.00
8	FF	0	5.11	0.0538	97.2	4.54
8	FF	1	5.09	0.0564	92.6	4.33
8	FF	2	5.11	0.0567	92.6	4.33
8	FF	4	5.11	0.0601	87.1	4.07
8	BTREE	0	6.08	0.0568	110.0	5.14
8	BTREE	1	6.15	0.0581	109.4	5.11
8	<b>BTREE</b>	2	6.17	0.0604	105.7	4.94
8	BTREE	4	6.18	0.0625	102.3	4.78
16	FF	0	5.48	0.0546	102.8	4.81
16	FF	1	5.55	0.0559	102.1	4.77
16	FF	2	5.51	0.0584	97.2	4.54
16	FF	4	5.63	0.0613	94.5	4.42
16	BTREE	0	6.92	0.0587	121.4	5.67
16	BTREE	1	7.26	0.0617	122.0	5.70
16	<b>BTREE</b>	2	7.30	0.0627	120.9	5.65
16	BTREE	4	7.47	0.0669	116.2	5.43

Table 6: Fine-tuning separate layers in the draft model with LoRA can increase the acceptance rate and speed up BTree MTPCs for n=16 and one LoRA layer by 5.70 over STP on an RTX 3090 GPU. Nevertheless, the increased acceptance rate comes at increased latency, making further throughput boosts via more LoRA layers unviable for EvaByte. We shade the STP baseline in gray and ablated models trained for the additional epoch without LoRA in brown. Interestingly, for the L40S in Table 3, we still got improvements with two LoRA layers, which highlights the importance of carrying out such an analysis across devices.

Table 7: Most Successful HMM Configuration

Parameterisation		Transit	ion Type	Initialisation	
Contextual	Non-Contextual	Homogeneous	Inhomogeneous	Identity Init.	Uniform Init.
<b>√</b>	Х	Х	✓	✓	Х

#### E HIDDEN MARKOV MODELS SETUP

In our experiments we use **contextual**, **inhomogeneous** hidden Markov models (HMMs) with **identity initialisation** (see Table 7). We chose the above after preliminary experiments where we assessed the following configuration choices for training our HMMs.

**Parameterisation** We can parameterise HMMs to either be contextual, i.e. we can make the transition probabilities depend on the input, or we can make the transition probabilities be independent of the input (non-contextual).

**Transition Type** The transition matrix can be the same at each time step (homogeneous) or it can be different (inhomogeneous). The former would correspond to additional parameter sharing across sum layers in the circuit representation.

**Initialisation** A crucial setup is to initialise the HMM with transition matrices that are identity matrices, which make the HMM equivalent to CP at the beginning of training. We achieve this by adding a bias term to allow the HMM model to be initialised to identity matrices. This setting in combination with extending to larger token windows, i.e. n=16 lead to a scenario where HMMs outperform CP. The other alternative is to initialise the transition matrices uniformly at random (before softmax), but this complicates learning and yields performance that is lower than CP models.

#### F FURTHER EXPERIMENTAL DETAILS

To make the comparison between methods fair, we: a) constrained the models to not produce end-of-sequence symbols during generation, as the latency of retrieving KV cache items from memory increases with sequence length (Nawrot et al., 2024) and b) we filtered the validation set of the models to only include examples with both prompts and responses in English, as acceptance rates may vary dramatically based on the language chosen for the response.

We compute throughput by generating answers to 250 prompts and report the mean and std of 3 runs with different prompts.

## G ALTERNATIVE LOSSES

In early versions of this work we also experimented using a Kullback-Leibler divergence (KL) loss as recommended by Basharin et al. (2025). However, we found that training with the KL loss doubled the training time while requiring a lot more memory, and the benefits in acceptance rate did not outweigh the additional complexity. For completeness we include the loss below. **KL Loss**  $\mathcal{L}$ 

$$\mathcal{L} = \sum_{j=1}^{n} \mathcal{L}_{j} \gamma^{j-1}, \quad \mathcal{L}_{j} = \sum_{i=1}^{N} \sum_{t=1}^{L} \frac{f_{\text{KL}} \left( p_{\theta}(x_{t+j}^{(i)} \mid \mathbf{x}_{< t+j}^{(i)}) \middle\| q_{\theta'}(x_{t+j}^{(i)} \mid \mathbf{x}_{< t+j}^{(i)}) \right)}{N \text{valid}(i, j)}$$
(5)

In the above we condition both the draft model,  $q_{\theta'}$ , and the target model,  $p_{\theta}$ , on the gold data. The above is equivalent to the KL term from the word-level distillation loss in (Kim & Rush, 2016). 10

# H FURTHER RELATED WORK

MTP for byte-level LLMs Gloeckle et al. (2024) and Zheng et al. (2025) both pretrain byte-level LLMs which predict n=8 future bytes. This window size was found to be optimal for downstream

<sup>&</sup>lt;sup>10</sup>While performing sequence-level distillation, *i.e.*, conditioning on data sampled from the teacher model may improve distillation (Kim & Rush, 2016), we did not explore this.

performance in Gloeckle et al. (2024). Both make conditional independence assumptions, but the approaches are architecturally different. Gloeckle et al. (2024) uses a transformer head per token to provide different feature vectors to each head and uses a shared unembedding matrix. On the other hand, Zheng et al. (2025) uses a shared feature vector across heads with different unembedding matrices per token.<sup>11</sup> However, they only focus on greedy self-speculative decoding, while in our work, we also explore speculative sampling.

**Speculative Decoding with MTP drafts** Previous MTP work either ignores speculative sampling and only focuses on greedy self-speculative decoding (Gloeckle et al., 2024), or abandons guarantees altogether (possibly at the expense of quality): specifically, Cai et al. (2024) and Zheng et al. (2025) use a tree decoding mechanism to consider multiple candidates at each speculative decoding step. Since their approach may accept multiple continuations but only generate the longest accepted one, they bias the distribution and break the guarantees. Wang et al. (2024) use a subword-level draft model to speed up their byte-level STP model via speculative decoding. Most prior work has introduced sequential dependencies in the draft model through architecture modifications. Hydra (Ankner et al., 2024) modifies the Medusa heads such that the predicted probabilities are also a function of the input embeddings of predicted draft tokens. Eagle (Li et al., 2024) introduces sequential dependencies by autoregressively predicting future feature representations. While these works relax the independence assumption, they have no explicit probabilistic model for the dependencies introduced.

An exception is Basharin et al. (2025), who study the effect of relaxing the conditional independence assumption by using a CP factorisation. While they obtain some first promising results, showing that increasing the rank can increase the acceptance rate of tokens for speculative decoding, they focus on subword-level models which have very large vocabulary sizes (e.g.  $v \ge 100$ k). This makes CP very expensive, both in terms of the number of parameters needed, and the GPU memory required. Moreover, they evaluate their models on unrealistic scenarios, i.e. datasets used for pre-training LLMs rather than instruction fine-tuning. Finally, despite the fact that a lot of previous work exists on MTP for subword-level LLMs, they use different models from those widely used for benchmarking speculative decoding methods, despite the existence of a benchmark, Spec-Bench (Xia et al., 2024) and common models (e.g. Vicuna). In our case, since there is a limited amount of work on MTP for byte-level LLMs (Gloeckle et al., 2024; Zheng et al., 2025), we directly compare with the results of the EvaByte model.

There has been increasing interest in multi-token prediction not only for generation speed-up, but also for improved model performance on tasks due to the lookahead offered by MTP. For example, DeepSeek-AI et al. (2024, Table 4) show that MTP for a token window of 2 tokens leads to improvements in benchmark metrics even when MTP is not used at inference time. Furthermore, they report an increase in the throughput of the model by  $\times 1.8$  when using speculative decoding.

**Token granularity** In MTP a token can vary in granularity from bytes (Zheng et al., 2025) to subword tokens provided by tokenisers (Basharin et al., 2025).

In addition to the choice of token granularity, there are generally 3 axes related works differ on:

- Training from scratch vs distilling an existing STP model into a MTP model
- Neural network architectures for the token heads (e.g. Linear, MLP, Transformer)
- Probabilistic modelling assumptions (conditional independence vs more expressive models)

#### H.1 DIFFERENCES IN SCENARIO

**Training from Scratch** Evabyte (Zheng et al., 2025) train a MTP byte-level model from scratch using n = 8.

**Retrofitting STP to MTP** Some works explore both training from scratch and retrofitting an STP model into an MTP one (Cai et al., 2024; Basharin et al., 2025). In our work, we focus on the second setting.

<sup>&</sup>lt;sup>11</sup>It is worth noting that Gloeckle et al. (2024) also do an ablation in the appendix and find that linear heads were competitive.

# H.2 DIFFERENCES IN ARCHITECTURES

**Linear Heads** Basharin et al. (2025) use a linear parameterisation for each token head in their distillation experiments.

MLP Heads Cai et al. (2024) use a MLP with a single hidden layer for each output token head. Ankner et al. (2024) extend this to multiple layers of MLPs per output token. Gloeckle et al. (2024) make the heads context-aware by including a transformer head in each token head.

**Autoregressive Head** While the main point of having future token heads is to avoid the expensive autoregression of the target model, current state of the art speculative decoding models rely on "cheap" autoregression. Eagle (Li et al., 2024), which is the best performing on the speculative decoding benchmark, Spec-bench (Xia et al., 2024), fits an autoregressive model to predict future feature vectors of the model (i.e. the inputs to the softmax layer). A similar architecture was also used for the DeepSeekV3 model (DeepSeek-AI et al., 2024).

MLP Heads Cai et al. (2024) propose the Medusa model which uses a MLP with a residual connection for each token head. While in theory they could use many MLP layers, they choose to use MLPs with single hidden layer. Ankner et al. (2024) explore using deeper MLPs for each token head.

**Transformer Heads** Gloeckle et al. (2024) use a shared unembedding matrix and use a separate transformer for each token head. More precisely, in order to predict the token at offset s, i.e.  $x_{t+s}$ , they compute softmax ( $\mathbf{W}\mathbf{z}_s$ ), where  $\mathbf{z}_s$  is produced by a separate transformer head for each s, i.e.  $\mathbf{z}_s = H_s(\mathbf{x}_{\leq t})$ .

Sharing the Unembedding layer. While the decoding of Zheng et al. (2025) is based on Medusa, instead of using a MLP for each token head, they use a different unembedding matrix per token head. This modelling choice is possible due to the small vocabulary size of byte-level models, i.e.  $|\mathcal{V}|=320$ . In their training from scratch scenario, Basharin et al. (2025) use different unembedding layers  $\mathbf{W}_a^{(s)}$  in order to predict  $x_{t+s}$  for the mixture component with index a. As such, they parameterise  $s \times |a|$  unembedding matrices. This seems non-ideal, since the last layer in LLMs can have a large number of parameters, i.e.  $(V \times d)$ . In their distillation scenario they use a shared unembedding matrix.

 $<sup>^{12} \</sup>texttt{https://github.com/OpenEvaByte/evabyte/blob/98d5f48d32197b803e7560a798da35c7a4bdcf4d/evabyte\_hf/modeling\_evabyte.py\#L753}$